Journal of Biomolecular NMR, 4 (1994) 17–34
ESCOM

J-Bio NMR 147

Unusual conformation of a 3'-thioformacetal linkage in a DNA duplex*

Xiaolian Gao and Peter W. Jeffs

Structural & Biophysical Chemistry, Glaxo Inc., Research Institute, Research Triangle Park, NC 27709, U.S.A.

Received 4 May 1993
Accepted 2 July 1993

Keywords: 3'-Thioformacetal-linked oligonucleotide; NMR solution structure; Local conformation at ODN modification site; O4'-endo sugar conformation

SUMMARY

The DNA · DNA duplex d(CGCGTT$_{SCH_2O}$TTGCGC) · d(GCGCAAAACGCG) (designated duplex III) containing a 3'-thioformacetal (3'-TFMA) linkage in the center of the sequence was characterized in detail by two- and three-dimensional homonuclear NMR spectroscopy. The NMR results were analyzed and compared with those of two duplexes of the same sequence: One is an unmodified reference sequence and the other contains a formacetal (OCH_2O) linkage at the central T^T step (designated duplex I and duplex II, respectively). In general, the NMR spectra of duplex III closely resemble those of the analogous duplexes I and II, suggesting an overall B-type structure adopted by the 3'-TFMA-modified duplex III. Nonetheless, the detection of several distinct spectral features originating from the protons at the T6$_{3'\text{-}SCH_2O}$T7 modification site is indicative of a local conformation that is clearly different from the corresponding region in duplexes I and II. The 3'-thioformacetal linker, in contrast to the formacetal (FMA) linkage, cannot be accommodated in a conformation usually found in natural nucleic acid duplexes. As a consequence, the 3'-TFMA-modified T6 sugar adopts an O4'-endo form (an intermediate structure between the usual C2'-endo and C3'-endo forms). This change is accompanied by a change in the ε (C4'-C3'-S3'-CH_2) dihedral angle and by subsequent adjustments of other torsion angles along the backbone. Notably, this conformational readjustment at the T6-T7 backbone linkage is localized; its collective result has negligible effect on base–base stacking of the T6 and T7 residues. A close examination of the COSY data in all three duplexes reveals a subtle variation in sugar geometry, with more S-type character adopted by the modified duplexes II and III. The results of this study illustrate that, although the difference between FMA and 3'-TFMA linkages is merely in the substitution of the T6(O3') in the former by a sulfur atom in the latter, the stereoelectronic difference in a single atom can induce significant local structural distortion in an otherwise well-structured oligonucleotide duplex.

INTRODUCTION

The search for modified oligonucleotides (ODNs) with enhanced nuclease stability and

*Supplementary material available from the authors: One table containing $J_{1'2'}$, $J_{1'2''}$ and $J_{3'4'}$ of duplexes I, II and III.

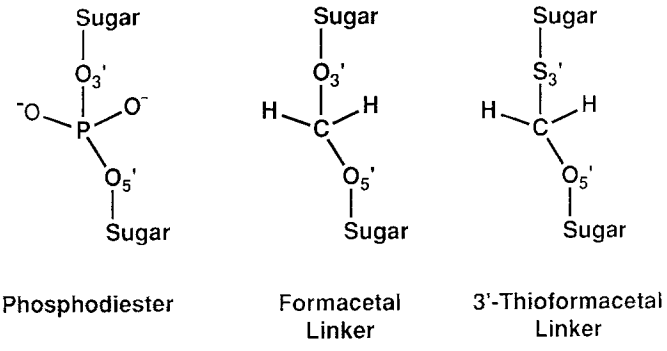

Fig. 1. Chemical structures of the backbone linkers, exemplifying the phosphodiester, formacetal and 3'-thioformacetal units.

improved cell permeability is an area of intense activity. This has led to a series of analogs where the phosphodiester linkage has been replaced by a nuclease-stable surrogate. One such series of analogs, exemplified by phosphorothioates, phosphoramidates and methyl phosphonates, has been prepared and shown to hybridize effectively to their target sequences and to exhibit enhanced nuclease stability (Uhlmann and Peyman, 1990). Unfortunately, this class of analogs suffers a major disadvantage, resulting from the creation of chirality at the phosphorus atom which leads to complex mixtures of 2^N diastereomers, where N is the number of modified linkages in the ODN.

To avoid the complexity that results from the introduction of these chiral phosphodiester linkages, a second generation of modified ODNs is emerging, where the phosphodiester is replaced by a neutral, achiral group (Matteuchi, 1990, 1991; Matteuchi et al., 1991). One recent addition to this latter series of linkers are ODNs containing an acetal moiety. The first reported example utilized the formacetal (FMA) group, which was inserted as a $T_{OCH_2O}T$ dimer block into deoxyoligonucleotide sequences. These chimeric ODNs were shown to form heterogeneous duplexes (Matteuchi, 1990; Veeneman et al., 1990, 1991) which exhibited slightly reduced thermal stability as compared to the unmodified sequences. Recently, an oligonucleotide sequence containing 5'-thioformacetal linkages (OCH_2S) was investigated in triplex formation. Its binding affinity, revealed by a thermal denaturation (T_m) analysis, was found to be lower than that of the unmodified control sequence (Matteuchi et al., 1991).

Despite this result, it appears that incorporation of a 3'-thioformacetal (3'-TFMA) linkage into ODNs results in properties that are similar to the structurally related FMA-containing ODNs (Fig. 1). In this context it has been shown that oligonucleotides containing multiple 3'-TFMA backbone modifications readily form duplexes with their complementary RNA strands (Jones et al., 1993). Interestingly and importantly, the resulting 3'-TFMA-DNA · DNA duplexes exhibit lower T_m values than their 3'-TFMA-DNA · RNA counterparts. This seemingly conflicting behavior of 3'-TFMA-containing ODN sequences led to the present investigation with the goal to understand the structural basis of duplex formation involving the 3'-TFMA linker.

Abbreviations: COSY, correlated spectroscopy; DQF, double-quantum filter; EDTA, ethylenediaminetetraacetic acid; NOESY, nuclear Overhauser effect spectroscopy; TOCSY, total correlated spectroscopy.

We have reported a comparative NMR study of a dodecamer duplex containing a single FMA modification, d(CGCGTT$_{OCH_2O}$TTGCGC) · d(GCGCAAAACGCG) (duplex II), and its unmodified parent sequence, duplex I (Gao et al., 1992). Our detailed analyses of these latter duplexes revealed that the structural impact occasioned by the introduction of a single FMA linkage is subtle and mostly localized at the modification site. Interpretation of the NMR-derived distance-correlation data leads to the conclusion that the FMA OCH_2O moiety appears to adopt a backbone geometry similar to typical B-form DNA with the methylene CH_2 group assuming the conformation of the phosphate PO_2 moiety with only minor deviation in the backbone torsion angles. The remarkable similarity of the NMR spectra of duplexes I and II suggests that the sugar pucker and base stacking of duplex I closely resemble those of duplex II. Our results are in accord with two previously reported examples (Cruse et al., 1986; Heinemann et al., 1991) where X-ray crystallographic studies of the selfcomplementary phosphorothioate duplex *R*p-d($G_SCG_SCG_SC$)$_2$ (*R* chirality represents the phosphorothioate) and the selfcomplementary duplex d($GCCCG_pGGC$)$_2$ containing a single 3'-methylene phosphonate linkage demonstrate that the structural consequence of these simple backbone modifications for a normal DNA framework is negligible. However, it should be realized that the reported studies represent only a limited number of examples and, before generalization can be made, more varieties of backbone-modified analogs need to be examined to investigate the allowable range of nucleotide backbone flexibility.

In the following, we describe two- and three-dimensional (2D and 3D) homonuclear NMR studies of a 3'-TFMA-containing duplex III, d($C_1G_2C_3G_4T_5T_{6SCH_2O}T_7T_8G_9C_{10}G_{11}C_{12}$) · d($G_{101}C_{102}G_{103}C_{104}A_{105}A_{106}A_{107}A_{108}C_{109}G_{110}C_{111}G_{112}$). In this dodecamer duplex, the O3' of T6 is substituted by a sulfur atom to give a 3'-TFMA T6–T7 linkage.

MATERIALS AND METHODS

Synthesis of 3'-TFMA duplex III

The unmodified strand d(GCGCAAAACGCG) was obtained by application of phosphoramidite chemistry on a 30 μM scale with an ABI 380B DNA synthesizer (McBride and Caruthers, 1983). A two-stage HPLC purification method was employed. Chromatography on PRP-1 (Hamilton, A: 0.1 M TEAA, pH 7.0; B: CH_3CN, 5–80% B over 50 min) for selecting trityl-positive material was followed by chromatography on a C_{18} column (Dynamax, 300 Å, 12 μm, 21 × 250 mm, A: 0.1M TEAA, pH 7.0; B: CH_3CN, 0–30% B over 50 min) after treatment with 80% aqueous acetic acid. The final product was desalted by a gel-exclusion sodium exchange column eluted with H_2O, and its sequence and base composition analyzed as described previously (Gao et al., 1992).

The 3'-thioformacetal ODN component of duplex III was provided by Dr. M. Matteucci (Gilead Sciences). Its synthesis was accomplished using standard solid-phase DNA chemistry, employing an H-phosphonate protocol (Froehler et al., 1986).

One- and two-dimensional NMR experiments

All NMR experiments were performed on a Bruker AMX 500 MHz spectrometer. Two complementary single strands, d(CGCGTT$_{SCH_2O}$TTGCGC) and d(GCGCAAAACGCG), when titrated at room temperature in aqueous buffer (pH 6.1), form duplex III as monitored by 1D proton spectra. The final NMR samples contained 2–3 mM of duplex in aqueous buffer (0.1 M

NaCl, 5 mM phosphate, 0.1 mM EDTA, pH 6.1). Proton 2D NMR spectra were collected in H_2O and D_2O. NOESY spectra with mixing times of 100 and 150 ms were obtained at 17 °C in H_2O solution. DQF-COSY, TOCSY (45 ms isotropic mixing time) and COSY-35 experiments, as well as NOESY experiments with mixing times of 100 and 250 ms, were performed at 30 °C in D_2O solution. A separate set of NOESY experiments (100 and 250 ms) were recorded at 17 °C. In all 2D NMR experiments, preacquisition delays varied between 1.5–2.0 s. NMR data matrices containing 2K complex data points in the t_2 dimension with a spectral width of 4504 Hz, and 512–1024 real points in the symmetrical t_1 dimension, were processed and analyzed using the FELIX program (Hare Research). Proton–proton distances were estimated from NOE connectivities on the basis of a two-spin approximation (Neuhaus and Williamson, 1989). Scalar coupling constants for sugar H1'-H2' and H1'-H2" proton pairs were measured from the antiphase separations of the COSY-35 cross peaks and sugar H3'-H4' couplings were estimated from both the magnitude and patterns of the COSY cross peaks. The ^{31}P spectrum was measured using 1D proton decoupling with a trimethyl phosphate sample in aqueous buffer solution (0.1 M NaCl, 10 mM phosphate, pH 6.2) as an external reference.

Three-dimensional homonuclear NOESY-TOCSY

This experiment was conducted in D_2O at 15 °C according to the protocol described previously (Gao and Burkhart, 1991). The 3D spectrum covered a spectral width of 8.06 ppm (4032 Hz) in each of the three dimensions, and was recorded with a NOE mixing time of 150 ms, followed by 25 ms of isotropic mixing. The dataset consisted of $512 \times 54 \times 105$ complex points in the $\omega_3/\omega_2/\omega_1$ dimensions, respectively. Data processing was carried out with the FELIX program; a 90° shifted sine-bell function was applied to all three dimensions. The t_3 dimension was baseline corrected by applying a fifth-order polynomial function and the final matrix contained $512 \times 256 \times 256$ data points. The 3D data was analyzed mainly through the planes of interest, which intersect with the ω_3 axis (ω_3 is a constant), because in this dimension the highest digital resolution was achieved.

Optical melting measurements

Thermal melting of duplex III was examined with Gilford Response II and Varian Cary IV UV spectrophotometers. A portion of annealed sample of duplex III used for NMR measurements was diluted with the same buffer as that used for NMR experiments to give adsorptions of 0.7–1.1 OD at 260 nm in a 1 cm cell. The temperature was increased from 10–90 °C and then decreased at a rate of 0.5 °C per min, and the observed melting curves were corrected from a blank buffer sample. The reported T_m is an average of those derived from the first derivative of three repetitive melting curves.

RESULTS

Temperature dependence of exchangeable imino protons and optical thermal melting behavior

Major exchangeable protons, such as imino protons of guanosine and thymidine residues and amino protons of cytidine residues were all assigned (Table 1) by following connectivities of dC(H6)-dC(H5)-dC(amino)-dG(imino), T(H6)-T(methyl)-T(imino), $dA(H2)_i$-$T(imino)_j$ and $dA(H2)_i$-$T(imino)_{i+1}$ (i and j are residue numbers from a complementary base of the opposite strand). Among these, dC(H6)-dC(H5) and T(H6)-T(methyl) are through-bond correlations

assigned from COSY spectra, while the rest are distance connectivities observed in NOESY spectra recorded in H_2O. These chemical shifts and their relative NOE intensities are typical of a Watson–Crick base-paired right-handed duplex (Wüthrich, 1986; Patel et al., 1987; Reid, 1987). It is noticeable that under similar conditions the imino proton resonances of the T5 and T6 residues (13.92 and 13.84 ppm, respectively) are shifted upfield in duplex III as compared to those (13.99 and 13.85 ppm) in the FMA duplex II. The latter, in turn, are slightly shifted upfield as compared to those (14.01 and 13.90 ppm) in the unmodified duplex I. Using NMR, we recorded the temperature profile of the imino proton resonances; some of the slices related to the central $(T \cdot A)_4$ block of duplex III are represented in Fig. 2. This set of data illustrates that the characteristics of the melting process of duplex III are similar to what was observed for duplexes I and II, where melting was initially accompanied by the upfield shift of the imino protons of the T5 and T6 residues and was cooperative, i.e. *no premelting at the modified T6-T7 site was observed.* The temperature effect on line widths has been used to compare spectra of the 3'-TFMA duplex III and the

TABLE 1
CHEMICAL SHIFTS OF THE 3'-THIOFORMACETAL DNA · DNA DUPLEX III[a]

	HN	NH_2	H8	H2	H6	H5	H1'	H2'	H2"	H3'	H4'	H5',H5"	HP1,HP2[b]
dC1					7.50	5.78	5.66	1.83	2.29	4.59	3.95	3.60	
dG2	12.98		7.83				5.80	2.58	2.61	4.85	4.22		
dC3		8.25,6.35			7.22	5.26	5.59	1.93	2.30	4.73	4.08		
dG4	12.82		7.79				5.91	2.55	2.71	4.87	4.29		
T5	13.92				7.14	1.33	5.91	2.06	2.52	4.75	4.15		
T6	13.84				7.37	1.51	5.96	2.22	2.58	3.63	4.04	3.94,4.13	
T7	13.81				7.34	1.52	5.94	1.95	2.50	4.64	4.13	3.67,4.05	4.96,4.99
T8	13.57				7.22	1.56	5.71	1.96	2.36	4.78	4.03		
dG9	12.55		7.76				5.71	2.50	2.56	4.88	4.24		
dC10		8.23,6.33			7.19	5.23	5.59	1.82	2.23	4.70	4.04		
dG11	13.05		7.77				5.82	2.48	2.60	4.85	4.22		
dC12					7.32	5.33	6.06	2.04	2.09	4.38	3.93	4.10	
dG101			7.83				5.86	2.47	2.66	4.74	4.12	3.60	
dC102		8.37,6.46			7.29	5.28	5.64	1.97	2.32	4.76	4.07		
dG103	12.89		7.76				5.77	2.49	2.60	4.87	4.23		
dC104		8.29,6.28			7.16	5.29	5.33	1.70	2.09	4.67	3.98		
dA105			8.03	7.07			5.64	2.54	2.68	4.90	4.22		
dA106			7.93	6.91			5.64	2.45	2.68	4.90	4.26		
dA107			7.85	6.93			5.71	2.41	2.69	4.88	4.27		
dA108			7.84	7.47			5.90	2.36	2.67	4.85	4.29		
dC109		7.86,6.32			6.97	4.94	5.45	1.70	2.14	4.66	4.00	4.11	
dG110	12.80		7.70				5.73	2.47	2.56	4.85	4.21		
dC111		8.35,6.50			7.19	5.28	5.65	1.78	2.20	4.70	4.04		
dG112			7.81				6.04	2.49	2.25	4.56	4.05	3.95	

[a] Data for exchangeable protons are from a 150 ms mixing time NOESY recorded in 0.1 M NaCl, 5 mM PO_4 and 0.1 mM EDTA, 290 K, pH 6.1, with chemical shifts referenced to that of the HOD resonance ($\delta = 4.78$ ppm). Data for nonexchangeable protons are from a 250 ms mixing time NOESY recorded at 303 K with chemical shifts referenced to that of the HOD resonance ($\delta = 4.58$ ppm).

[b] The 3'-thioformacetal methylene protons are T7(HP1, HP2). Their chemical shifts at 290 K are 4.91 and 5.02 ppm, respectively.

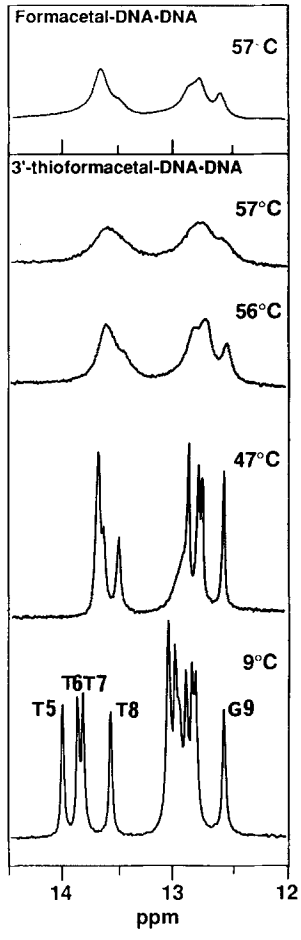

Fig. 2. 1D NMR temperature profile of the imino protons of the 3'-TFMA duplex III (lower four slices) compared to the imino-proton spectrum of the FMA duplex I at 57 °C (top slice). These spectra were acquired in H_2O under the conditions described in the text and each spectrum was recorded with minimal 10 min of equilibration time.

FMA duplex II (Fig. 2). Between 56–57 °C, all imino resonances of duplex III quickly broadened, with the spectrum at 56 °C closely resembling that of duplex II at 57 °C. The first derivative of the UV melting profile of duplex III gave an average T_m of 48.8 °C. Under the same conditions, the unmodified duplex I and the FMA duplex II produced T_m values of 53.0 and 50.0 °C, respectively.

Proton and NOE assignments

All nonexchangeable proton resonances, except for those of H5' and H5", were assigned by analyzing various NMR spectra acquired in D_2O (Table 1). Well-connected intraresidue and sequential NOEs were observed between base and sugar protons. This is illustrated in Fig. 3, which displays the through-space connectivities of base (6.8–8.2 ppm) to sugar H1' protons (5.2–6.2 ppm). This spectral region contains four different types of NOEs: the intra- and interresidue NOEs linking base and sugar H1' protons (cross peaks connected by the solid and dashed

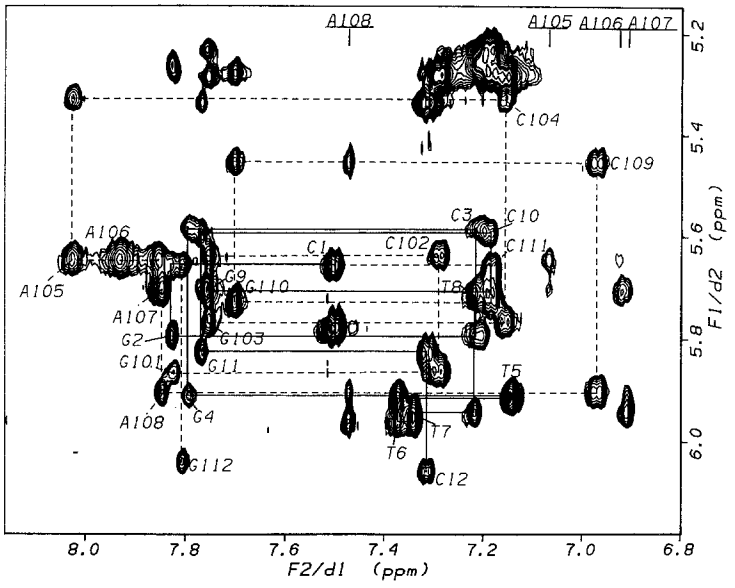

Fig. 3. Expansion of a NOESY spectrum of duplex III (250 ms mixing time, recorded at 30 °C) in the region of base (6.8–8.2 ppm) and H1' (5.2–6.2 ppm) resonances. Intraresidue and sequential NOEs are demonstrated by connected solid and dashed lines for each of the strands. NOEs related to adenosine H2 protons are visible through their labeled resonances.

lines); the intra- and interstrand NOEs linking adenine H2 and sugar H1' protons (cross peaks aligned along the F1 axis at each labeled adenine H2 frequency); the sequential NOEs linking the purine $(H8)_i$ with pyrimidine$(H5)_{i+1}$ protons (cross peaks located in the regions of F2: 7.7–7.9 ppm and F1: 5.2–5.4 ppm); and the strong intraresidue NOEs between dC(H6) and dC(H5) resonances (mostly located in regions of F2: 7.1–7.4 ppm and F1: 5.2–5.4 ppm). The majority of the chemical shifts (Table 1) and NOE connectivity patterns in duplex III are quite comparable to what we described previously for the FMA duplex II and the unmodified duplex I, suggesting that overall structural features, such as base stacking, base–base and cross-strand separations, are similar in these three duplexes.

COSY spectra and coupling constants

An expanded COSY-35 spectrum containing scalar coupling connectivities from H1' (5.3–6.1 ppm) to H2' and H2" (1.6–2.8 ppm) protons is shown in Fig. 4. The antiphase character of cross peaks in this and similar examples was found particularly useful for identifying overlapped purine H2' and H2" resonances. Each pair of H1'-H2' and H1'-H2" protons in duplex III was unambiguously assigned. Additionally, the antiphase components permitted the measurement of $J_{1'-2'}$ and $J_{1'-2''}$ coupling constants within an accuracy of ± 0.5 Hz (Fig. 4 and Table S1) and provided a good estimation for $J_{3'-4'}$ and $J_{3'-2'}$, $J_{3'-2''}$ (Table S1). A comparison of the coupling constants $J_{1'-2'}$ and $J_{1'-2''}$ for all three duplexes, i.e. the unmodified duplex I, the FMA duplex II and the 3'-TFMA duplex III is plotted in Fig. 5, along with a reference plot for coupling constants $J_{1'-2'}$ and $J_{1'-2''}$ in standard C3'-endo, O4'-endo and C2'-endo conformations. This set of data provides a basis for assessing the sugar conformational transition.

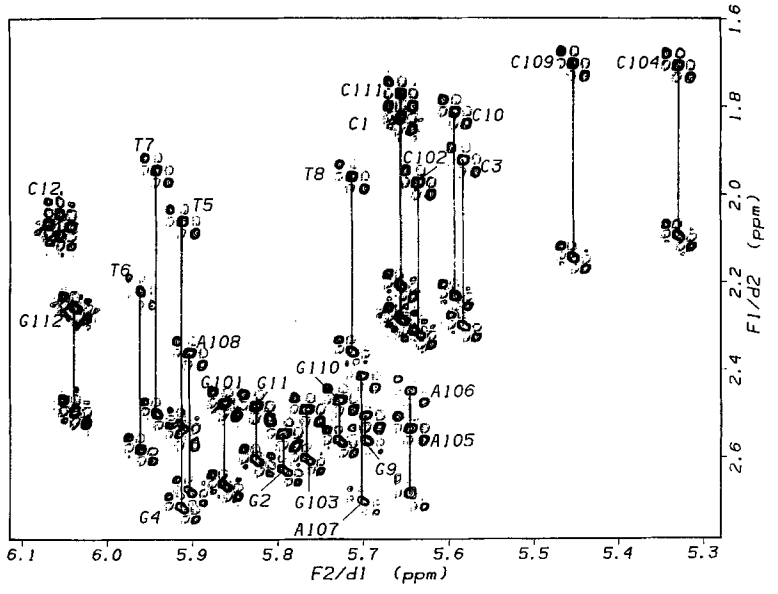

Fig. 4. Expanded COSY-35 spectrum, recorded at 30 °C illustrating the region containing the H1' (5.3–6.1 ppm) and H2',H2" (1.6–2.8 ppm) resonances. Antiphase character of these cross peaks is reflected by intensities of the lines. All H1'-H2' and H1'-H2" coupling correlations in duplex III are exemplified.

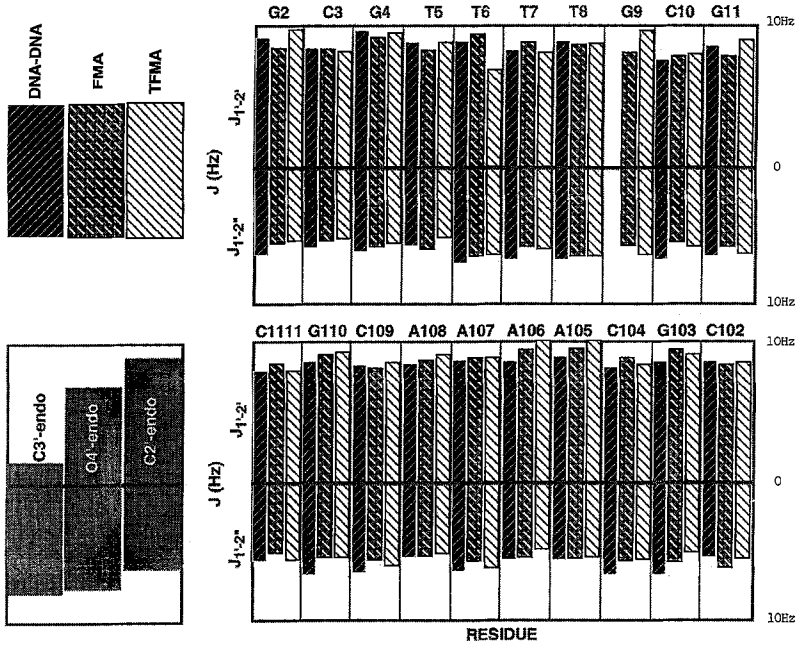

Fig. 5. Comparison of $J_{1'-2'}$ and $J_{1'-2''}$ of the unmodified duplex I (left bar for each residue), the FMA duplex II (middle bar) and the 3'-TFMA duplex III (right bar) for the central 10 residues. Coupling constants were measured from COSY-35 spectra and their values are listed in Table S1. The ideal $J_{1'-2'}$ and $J_{1'-2''}$ couplings of standard sugar puckers are plotted in the lower left corner.

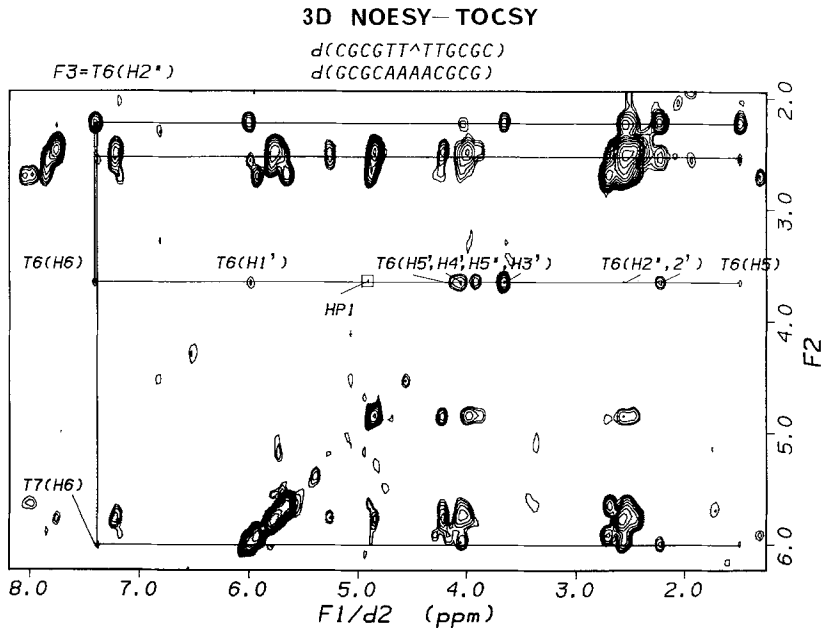

Fig. 6. Expanded 2D plane viewed at the frequency of T6(H2') (2.22 ppm) at the F3 axis in the 3D NOESY-TOCSY spectrum (150 ms mixing time) recorded at 15 °C in D_2O. The connectivities of the lines parallel to the F1 axis are as follows: F2 = 2.22 ppm is a TOCSY line where all cross peaks are equivalents of their 2D counterparts; F2 = 2.58 ppm is from the J-coupled T6(H2')-T6(H2''), NOE connectivities from T6(H2'') to other protons can be identified along this line; F2 = 3.63 ppm is from the J-coupled T6(H2')-T6(H3') and illustrates the NOE connectivities from T6(H3') to other protons along this line; F2 = 5.96 ppm is from the J-coupled T6(H2')-T6(H1') and identifies the NOE connectivities from T6(H1') to other protons that fall on this line. The boxed weak cross peak is assigned to a NOE from T6(H3') to a 3'-TFMA methylene proton; its intensity is weaker than that of the T6(H3')-T6(H1') cross peak.

3D NOESY-TOCSY spectrum

The major application of the 3D spectrum of duplex III was to resolve overlaps of some critical resonances in the 2D NOESY spectra and to verify ambiguous assignments in order to improve distance estimates. For example, although there are two sets of 2D data, recorded at 17 and 30 °C respectively, from which it was possible to conclude that T6(H3') resonates at 3.63 ppm, it was essentially impossible to separate the NOEs associated with this proton from those of near-isochronous resonances (Table 1). This was particularly true for resonances related to T7 (H5') at 3.67 ppm, since many of the protons in residues T6 and T7 exhibit similar chemical shifts (Table 1). Shown in Fig. 6 is an expanded 2D plane of the 3D NOESY-TOCSY spectrum, viewed through T6(H2'), resonating at 2.22 ppm, where it is best resolved from T7(H2') resonating at 1.95 ppm. Three horizontal lines parallel to the F1 axis in this plane link cross peaks that were observed due to scalar coupling transfers from T6(H2') to H1', H2'' and H3' of T6 at 5.96, 2.58 and 3.63 ppm, respectively. On each of the three lines, normal NOE correlations, connecting these sugar protons to other sugar and base protons, were observed as displayed in Fig. 6. Most importantly, a weak NOE related to the interaction between T6(H3') and 3'-TFMA methylene protons was unambiguously assigned and its distance quantitated by referencing to the T6(H3')-T6(H1') cross peak. The relative contribution can be estimated by judging the intensity of the

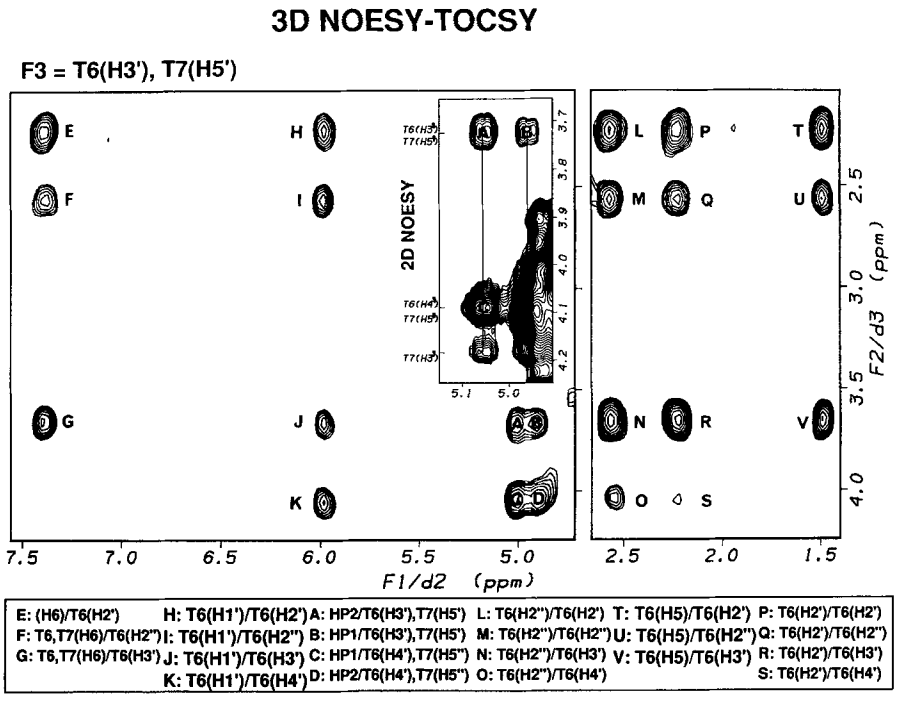

Fig. 7. Expanded 2D plane viewed at the frequencies of T6(H3') and T7(H5') (3.63 ppm) at the F3 axis in the 3D NOESY-TOCSY spectrum (150 ms mixing time) recorded at 15 °C in D_2O. All of the cross peaks are connected to the T6(H3') or T7(H5') protons through resonances on the F2 axis; their specific assignments in the F2 and F1 dimensions are listed under each column of cross peaks in the figure.

T6(H3')-(HP1) cross peak derived from the 3D data (HP1 and HP2 are TFMA methylene protons).

Figure 7 is a 2D plane from the 3D NOESY-TOCSY, sliced through 3.63 ppm where resonances T6(H3') and T7(H5') are partially overlapped. An insert of the expanded 2D NOESY plot in Fig. 7 permits comparison of the 3'-TFMA methylene proton-related NOE cross peaks A, B, C and D in a 2D spectrum with their counterparts in the 3D spectrum. Evidently, cross peak D, which is located in an extensively superimposed spectral region (F2 4.96 ppm; F1 4.12 ppm), is well resolved in the 3D spectrum (Fig. 7). Cross peaks A–D in the 3D dataset are due to proton–proton contacts of the 3'-TFMA methylene protons at 4.91 and 5.02 ppm with T6(H3') and T7(H5') (peaks A and B) and T6(H4') and T7 (H5") (peaks C and D).

Spectral features related to the 3'-thioformacetal linkage

Several distinctive spectral characteristics were observed, associated with the resonances in the vicinity of the 3'-TFMA modification site. The 3'-TFMA methylene protons were observed resonating at near-isochronous positions of 4.96 and 4.99 ppm at 30 °C. The small chemical-shift separation between these two protons was increased to 0.11 ppm (4.91 and 5.02 ppm) by lowering the temperature to 17 °C. Also, a distinctly different pattern of coupling cross peaks was observed for the sugar residue of T6 in the COSY-35 spectrum. $J_{1'-2'}$ and $J_{1'-2''}$ became comparable in

magnitude (both were measured at 6.7 Hz, Table S1 and Fig. 4) whereas unusual strong couplings were observed for $J_{3'-2'}$, $J_{3'-2''}$ (> 6 Hz) and $J_{3'-4'}$ (Fig. 8). A small change from the typical pattern (Chary et al., 1988) was discernible from the coupling cross peaks of the T7 sugar residue, which exhibited relatively strong coupling cross peaks for H3'-H2', H3'-H2" and H3'-H4' of T7 (Fig. 8).

NOEs related to the 3'-TFMA methylene protons are listed in Table 2. These assignments were derived from several NOESY datasets including 3D NOESY-TOCSY and 2D NOESY experiments recorded at different temperatures. The NOE intensities were determined by comparing relative intensities of the cross peaks in the same dataset and a few well-resolved cross peaks were used as a cross-reference between different datasets. The resonance overlap between the T6(H3') and T7(H5') protons and between the T6(H4') and T7(H5") protons (Table 1) introduced a complication. The T6(H3') and T7(H5') overlap was resolved by viewing 3D data through the frequency of T6(H2') as shown in Fig. 6, while the NOE assignments connecting the 3'-TFMA methylene protons with T6(H4') and T7(H5") protons were confirmed by 2D NOESY spectra at 17 and 30 °C, respectively. At 30 °C, T6(H4') resonates 0.01 ppm upfield and at 17 °C, 0.01 ppm downfield from T7(H5") (assignments based on TOCSY data). The corresponding partially overlapped NOE cross peaks correlating a 3'-TFMA methylene proton with T6(H4') (stronger) or T7(H5") (weaker), exchanged their positions in NOESY spectra at 30 °C, compared to that at 17 °C. Some NOEs listed in Table 2, such as those from the 3'-TFMA methylene protons to T6(H1'), T6(H2') and T6(H2") protons, may be due to spin-diffusion, and were observed only in a 250 ms mixing time NOESY experiment.

^{31}P spectrum

A 1D proton-decoupled ^{31}P spectrum of duplex III was recorded at 30 °C. All 21 phos-

TABLE 2
NOE ASSIGNMENTS IN FORMACETAL DUPLEX II AND 3'-THIOFORMACETAL DUPLEX III (ppm)

	T6(H3')	T6(H4')	T6(H1')	T6(H2')	T6(H2")	T7(H3')	T7(H5')	T7(H5")	T6(H5',H5")
Formacetal DNA · DNA[a,b]									
	4.48	4.02					4.22	3.53	
HP1 4.80	w		w−		w−		m−	m	
HP2 4.94	m		w−	w−	w	w−	w	w	
T7(H5')									
3'-Thioformacetal DNA · DNA[a]									
	3.70[c]	4.10[c]					4.08[c]	3.74[c]	
HP1 4.92[c]	w[d]	s	w−[e]	w−[e]	w[e]	w−[e]	w	w−	w[e]
HP2 5.05[c]	w−[d]	s−			w−[e]	w−[e]	m−	w	w−[e]
T7(H5')					w[e]				

[a] HP1/HP2 and H5'/5" sugar protons are not stereoassigned. However, the given relative intensities are consistent among these assigned NOEs. NOE cross-peak intensities are characterized in descending order by (s, s−, m, m−, w, w−). w and w− are also used for cross peaks observed only in the 250 ms NOESY spectrum. s: 1.8–5.0 Å; m: 2.5–5.0 Å; w: 3.0–5.0 Å.
[b] Data derived from 2D NOESY spectra recorded at 308 K (100 and 250 ms mixing times).
[c] 2D NOESY spectra recorded at 290 K (100 and 250 ms mixing times).
[d] 3D NOESY-TOCSY spectrum recorded at 288 K (150 ms NOE mixing time).
[e] 2D NOESY spectra recorded at 303 K (100 and 250 ms mixing times).

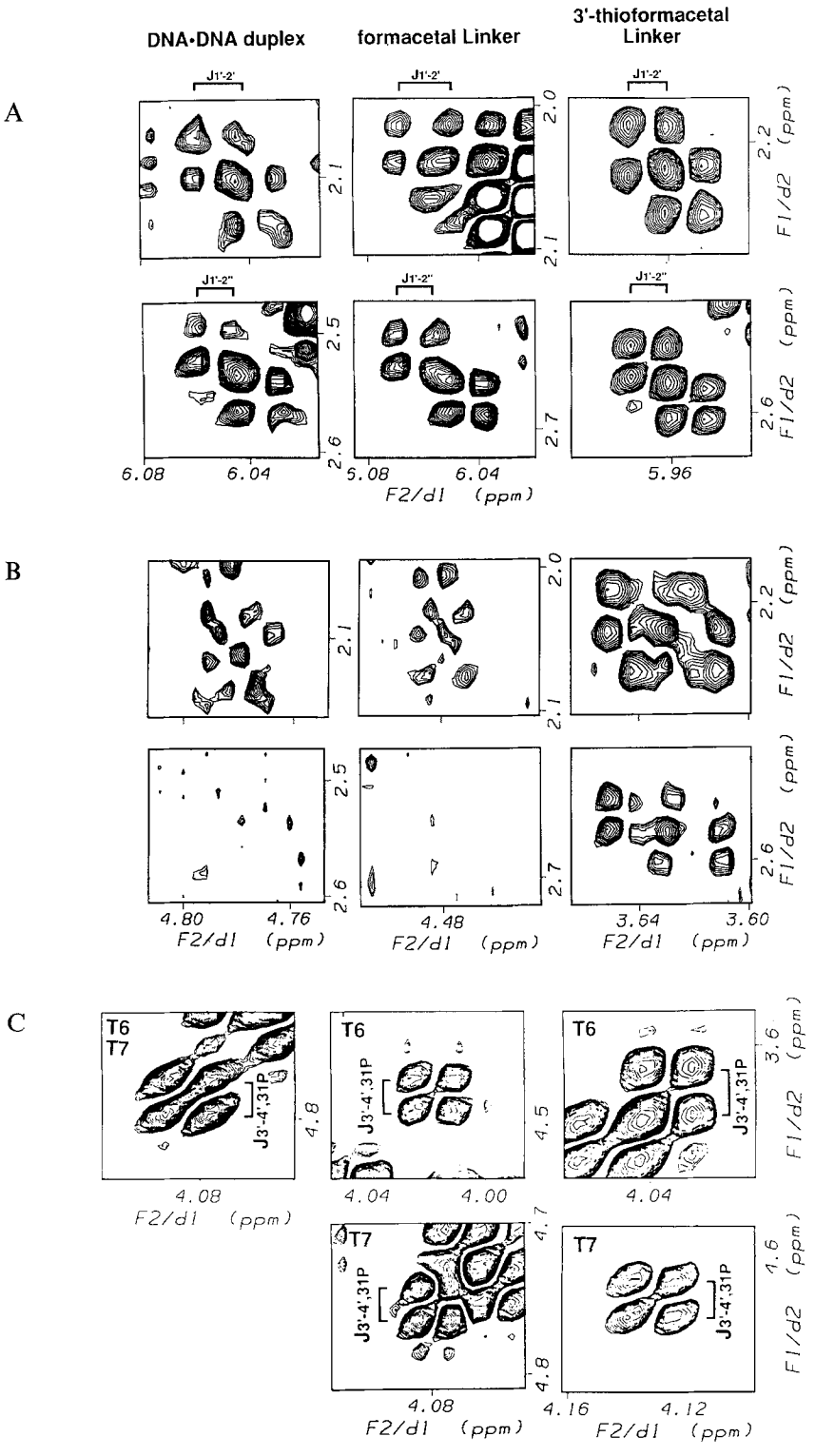
DNA•DNA duplex
formacetal Linker
3'-thioformacetal Linker
A
B
C
J1'-2'
J1'-2"
F1/d2 (ppm)
F2/d1 (ppm)
6.08
6.04
5.08
5.96
4.80
4.76
4.48
3.64
3.60
4.08
4.04
4.00
4.16
4.12
T6
T7
J3'-4',31P

phate resonances were observed in a narrow spectral region of 0.6 ppm, 3.9–4.5 ppm upfield from that of an external trimethylphosphate resonance. No unusual chemical shifts were detected.

DISCUSSION

This report is the second in a series of structural studies involving oligonucleotides containing backbone modifications. Previously we have reported on a method of progressive chemical structural perturbation to assess effects of incorporating an FMA linkage in an ODN on duplex formation (cf. duplex II). Here we describe the NMR results of the structural studies of 3'-TFMA duplex III in a similar comparative manner with respect to the unmodified duplex I and the FMA duplex II, with a focus on the local conformation at the modified T6-T7 site.

Structural features of duplex III

With the exception of the residues at the modification site, the overall structural features of the 3'-TFMA duplex III are consistent with a regular B-type helix and are similar, based on their NMR spectra, to those of unmodified duplex I and the FMA duplex II. Ten Watson–Crick base-paired imino proton signals were observed to account for the central ten base pairs. From the chemical shifts and NOE correlations of these marker signals, it is evident that no major disruption in base pairing and stacking occurs in duplex III. A more interesting aspect is to use the imino protons of the central $(T \cdot A)_4$ block as probes for microscopic melting behavior at the modification site. When duplex III was subjected to a temperature gradient from 9–57 °C, a similar NMR melting transition behavior, manifested in line broadening of the imino protons, as those reported for duplexes I and II was observed. The melting was preceded by the upfield shift of the T5 and T6 imino resonances; 'premelting' of the dG2 and dG111 imino resonances occurred as evidenced by significant broadening of the line widths of these signals at 57 °C (Fig. 2).

The NMR temperature-dependence data reflect the melting behavior of each individual base pair, whereas the optical melting is based on the change in hyperchromicity of bases that results from destacking. From a comparison of the temperature dependence of the spectra of duplexes III and II, we can conclude that the 3'-TFMA sequence melts one degree earlier than the FMA sequence (Fig. 2). This corresponds to a loss in energy of < 1 kcal/mol, a result that is consistent with the observations from optical measurements. These parallel results obtained by NMR and optical experiments suggest that the destabilization energy introduced by the 3'- TFMA linkage is dissipated along the sequence, rather than localized at a single site.

Structural details of duplex III were obtained by analyzing intraresidue and sequential proton–

←

Fig. 8. Expanded COSY-35 spectra of the unmodified duplex I (left panels), the FMA duplex II (middle panels) and the 3'-TFMA duplex III (right panels). All spectra were plotted with the same spectral width. (A) Cross peaks of H1'-H2' (top three panels) and H1'-H2" (lower three panels) of the T6 residue. The coupling cross-peak patterns of the 3'-TFMA duplex III are distinctly different from those of duplexes I and II. (B) Cross peaks of H3'-H2' (top three panels) and H3'-H2" (lower three panels) of the T6 residue. For duplexes I and II, coupling constants of H3'-H2" are too weak to be observed, while the corresponding coupling of the 3'-TFMA duplex III is obvious. (C) Cross peaks of H3'-H4' of the T6 residue (top three panels) and the T7 residue (lower three panels). $J_{3'4'}$ couplings of T6 and T7 in duplex III are larger than those in duplexes I and II.

proton separations and sugar puckers, derived from NMR spectra acquired in D_2O (Figs. 3 and 4, Table S1). The correlation patterns of base and sugar protons observed in the NOESY datasets are typical of a right-handed B-form duplex and are similar to the spectra of duplexes I and II presented previously. It is worth noting that in NOESY spectra of duplex III, we observed a similar set of cross peaks connecting adenosine H2 protons with adjacent and cross-strand sugar H1' protons as those found in duplexes I and II. The relative intensities of these NOEs increase from dA105(H2)-related cross peaks to dA108(H2)-related cross peaks (Fig. 3). This trend in increasing NOE intensities from 5'-dA to 3'-dA residues was attributed to a compression of the minor groove at the 3'-end of a dA_n tract (Katahira et al., 1988). Thus, the incorporation of a single 3'-TFMA linkage in the center of the dA_4-tract exerts negligible perturbation of the minor groove, which is characteristic of a sequence consisting of a string of continuous dA residues.

The high-resolution COSY-35 spectrum contains detailed information on conformational features, characterized by the type of sugar pucker through the fingerprint patterns which incorporate the antiphase peak splitting (Fig. 4). Although the COSY cross-peak patterns of all three duplexes appear to be consistent with S-type sugar, a close comparison suggests that small differences exist. As sugar conformation is progressively transformed from C3'-endo (N-type) through O4'-endo to C2'-endo (S-type), $J_{1'-2'}$ increases and $J_{1'-2''}$ slightly decreases; that is, more S-type character in a sugar residue is associated with a larger $J_{1'-2'}$ and a smaller $J_{1'-2''}$ (Fig. 5). Indeed, comparing $J_{1'-2'}$ and $J_{1'-2''}$ of duplexes I, II and III in order (Fig. 5), those from residues dC3, dG4, T7, T8, dC10 and dG11 in one strand and dG103, dC104, dA105, dA106, dA108, dC109 and dG110 in the second strand exhibited either progressively increased $J_{1'-2'}$ or decreased $J_{1'-2''}$ or both. These changes in sugar pucker are subtle but consistent. The observed trend is less apparent for $J_{3'-2'}$, $J_{3'-2''}$ and $J_{3'-4'}$. These measurements are less accurate due to either weak intensities and/or a multicoupling mechanism. These results suggest that introduction of a single modification, representing an FMA linker or 3'-TFMA linker, induces a change in the sugar conformational equilibrium towards one with more S-type character than is found in duplexes I and II, respectively. Moreover, while the cross-peak pattern variation is obvious in the COSY-35 spectrum, NOESY spectra are less sensitive to this minor structural variation.

Conformation of the modification site

In contrast to the FMA-containing oligonucleotides which exhibit a set of NMR parameters comparable to those of duplex I, representative of a typical B-form helix, introduction of a 3'-TFMA linkage results in several distinctive spectral features in duplex III which can only be attributed to backbone structures that deviate significantly from the geometries found in duplexes I and II.

Sugar pucker perturbation of 3'-TFMA-linked residues. In the COSY-35 spectrum of duplex III, J-coupling cross-peak patterns correlating T6 sugar protons varied significantly. A comparison of the patterns of these peaks ($J_{1'-2'}$, $J_{1'-2''}$, $J_{3'-2'}$, $J_{3'-2''}$, $J_{3'-4'}$) with the corresponding peak patterns of duplexes I and II (Fig. 8) demonstrates a clear trend with $J_{1'-2'}$ (T6) < $J_{1'-2'}$ (C2'-endo); $J_{1'-2''}$ (T6) ≈ $J_{1'-2''}$ (C2'-endo); $J_{3'-2'}$ (T6) > $J_{3'-2'}$ (C2'-endo); $J_{3'-2''}$ (T6) > $J_{3'-2''}$ (C2'-endo); and $J_{3'-4'}$ (T6) > $J_{3'-4'}$ (C2'-endo). While the observed variations in coupling constants cannot be explained by the electronegativity effect of the substituent (Haasnoot et al., 1980), the general direction of this shift in T6 coupling constants correlates well with the calculated J–P relation where P is a pseudorotation parameter derived from the torsion angles of furanose sugars in nucleosides

(Saenger, 1984). This points towards an equilibrium favoring the O4'-endo conformation, which is intermediate between a C2'-endo and C3'-endo conformation adopted by the T6 sugar moiety (Veal and Brown, 1992). A similar analysis of the couplings related to the T7 residue (Figs. 5 and 8) revealed that the sugar ring of T7 is less C2'-endo-like in duplex III than in duplexes I and II, although it is not quite in the O4'-endo range. In contrast, judging from coupling cross-peak patterns, the sugar conformation of the T5 residue remains C2'-endo-like in duplex III. We also discovered that the characteristics of the coupling cross peaks related to T6 in duplex III closely resemble its counterpart in a hybrid DNA · RNA duplex of the same sequence (Gao and Jeffs, 1993). The implication is that the reported destabilization of DNA · DNA duplexes and stabilization of DNA · RNA duplexes upon 3'-TFMA backbone modification may be attributed to the inability of a 3'-TFMA-modified sugar to assume a C2'-endo conformation.

Backbone conformation of the 3'-thioformacetal linker. The 3'-TFMA methylene protons that are directly linked to the T6(S3') resonate at 4.96 and 4.99 ppm in spectra obtained at 30 °C. For comparison, the T6(O3')-linked FMA methylene protons show more widely separated shifts at 4.80 and 4.94 ppm at 35 °C. As mentioned, the chemical shifts of 3'-TFMA methylene protons, in contrast to the FMA protons in duplex II, are sensitive to temperature variation, with increased separation of the methylene protons occurring with decreasing temperature (4.91 and 5.02 ppm at 17 °C). This observed temperature dependence associated with 3'-TFMA resonance frequencies reflects a softer, and thus more flexible, -S-CH_2-O- backbone in duplex III, which confers faster dynamics at elevated temperature as compared to the FMA O-CH_2-O- backbone in duplex II. Substitution of oxygen with a less electronegative sulfur is expected to induce an upfield shift in vicinal proton resonances. Consistent with this, we observed a strongly upfield shifted T6(H3') resonance at 3.63 ppm in the 3'-TFMA linker as compared to the corresponding signal at 4.48 ppm in the FMA duplex II. One of the T7(H5',5") resonances was shifted downfield in duplex III compared to duplex II (4.22/3.53 and 4.05/3.67 ppm in FMA and 3'-TFMA duplexes, respectively). Since chemically, these two groups of protons are subjected to the same change in environment upon sulfur substitution, the difference in chemical shifts likely originates from variations in their torsional geometry at the linker sites of duplexes II and III. Our NOE data analysis (vide infra) is consistent with this notion.

For the purpose of discussion of the NMR data as it pertains to local structural differences in the region of modification, stereoplots of an unmodified ssODN fragment (1) and its 3'-TFMA counterpart (2) are shown in Fig. 9. An interesting comparison of the NOEs related to the modification site in the 3'-TFMA duplex III and the FMA duplex II is listed in Table 2. While the majority of NOEs arising from the contacts between the linker methylene protons and adjacent sugar protons can be matched in these two duplexes, some appear to be different in relative intensities. For example, NOEs are present for HP2-T7(H5") and HP2-T6(H3') in duplex III as compared to HP1-T7(H5") and HP2-T6(H3') in duplex II. More important and of particular significance is the observation that in duplex III, strong NOEs occur between the linker methylene protons and T6(H4') and weak NOEs correlating T7(H5',H5") with the linker and T6(H2") protons (Table 2); these NOEs are absent in the FMA duplex II. Further analysis of these particular NOEs in duplex III revealed that the backbone torsion angles bridging the $T6_{SCH_2O}T7$ step have undergone significant readjustment. For example, distances between charged oxygens and the 5'-preceding H4' in a canonical nucleic acid duplex in either B- or A-type conformation are at least 4.8 Å. However, intense NOEs arising from close contact of T6(H4') and 3'-TFMA

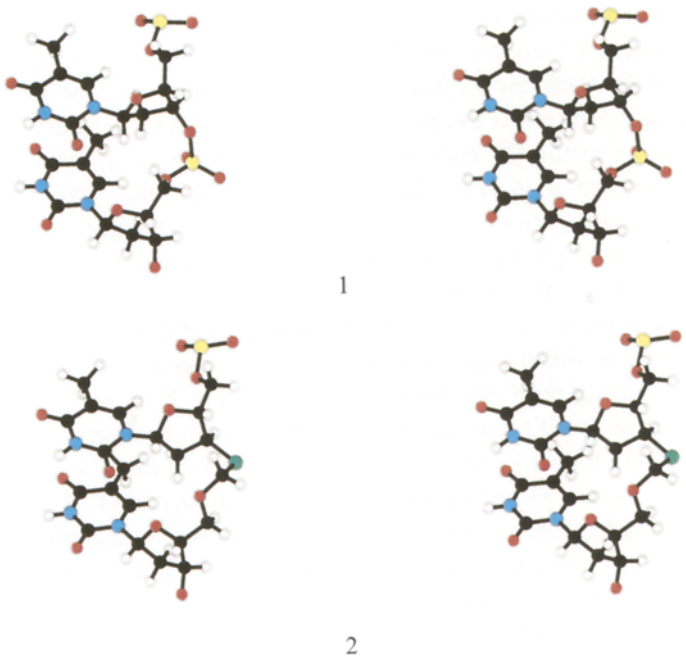

Fig. 9. Stereoplots showing a single-strand component between T6 and T7 of a model oligonucleotide duplex (structure 1) and a qualitative model derived from the NMR data of duplex II for the analogous structure containing the 3'-TFMA linker (structure 2).

methylene protons were detected in the 3D NOESY-TOCSY spectrum of duplex III (Fig. 7). Therefore, if a rotation of ~ 180° is applied to torsion angle ε (C4'-C3'-S3'-CH_2), the resulting geometry would satisfactorily explain the observed close contacts between methylene and T6(H4') protons, as well as the weak NOE connecting methylene with T6(H3') protons (Table 2, Fig. 6). We suspect that this change in torsion angle ε is triggered by the requirement of releasing the nonbonded interactions between the lone-pair electron on the sulfur atom and the C4' carbon of the sugar ring that is induced by O4'-endo sugar pucker. NOE data in Table 2 can be further rationalized if the rotation of the ε dihedral angle is considered to propagate in the 3'-direction to the following ζ, α, β and γ torsion angles as described in Table 3. Additionally, our estimation of the distribution of torsion angle γ being in the range 120–180° is supported by the large coupling constant observed for T7(H4')-T7(H5''), a negligible coupling for T7(H4')-T7(H5'), and a moderate NOE between H5' and H3' of T7 (Blommers et al., 1991).

Finally, it is interesting to point out that the crystallographic study of a 3'-methylene-modified duplex demonstrated that a local sugar conformational change occurs with a concomitant ~ 40° crankshaft rotation around the β-backbone link (Heinemann et al., 1991). The results from crystallographic and solution NMR studies of backbone-modified oligonucleotides indicate that the specifics and the nature of backbone reorganization are structural and sequence dependent.

CONCLUSIONS

In general, various NMR spectra of duplex III closely resemble those of its analogous duplexes

TABLE 3
ESTIMATED VALUES FOR BACKBONE TORSION ANGLES IN THE T6-T7 MOIETY OF DUPLEX III, COMPARED TO VALUES IN STANDARD B-DNA GEOMETRIES

	α	β	γ	δ	ε	ζ	χ
Duplex III	30–150	120–180	120–180	105	0–60	90–180	
B-DNA	−56	−171	51	140	−167	−103[a]	98(Y); 102(R)[a]
	−41	136	38	140	−133	−157[b]	
	−72	175	57	140	−91	151[c]	

Torsion angles are given in degrees.
[a] BI-geometry (Dickerson, 1983).
[b] Average B-geometry (Chandrasekaran et al., 1980).
[c] BII-geometry (Dickerson, 1983).

I and II, suggesting an overall B-type structure adopted by the 3'-TFMA-modified duplex III. Nonetheless, several distinct spectral features, originating from the protons at the $T6_{SCH_2O}T7$ modification site, indicate a local conformation that is clearly different from its counterparts in duplexes I and II. Specifically, in comparison to the FMA duplex II, differences in spectral parameters were reflected by (a) the large upfield shift (0.78 ppm) of the T6(H3') resonance; (b) differences in patterns and intensities of the NOE cross peaks connecting the 3'-TFMA methylene protons with the sugar protons of residues T6 and T7; and (c) deviations of the magnitude of the coupling constants and the coupling cross-peak patterns of the T6 and, to a lesser extent, T7 sugar moieties from those of a typical S-type sugar.

Collectively, these NMR parameters give strong indications that, in contrast to the FMA linkage, the 3'-TFMA linker cannot be accommodated in a conformation usually found in natural nucleic acids. Consequently, the T6-3'-TFMA sugar undergoes a conformational transition to the O4'-endo form (an intermediate between C2'-endo and C3'-endo) which is accompanied by the rotation of the ε dihedral angle and subsequent adjustments of other torsion angles along the backbone. Notably, this conformational readjustment at the T6-T7 backbone linkage is localized, with the result that it has negligible effect on base–base stacking between residues T6 and T7. This localized linker region of the modified strand of duplex III, as portrayed in structure 2 (Fig. 9), accounts in a qualitative manner for the NMR data. Additionally, the results of this study provide an example which illustrates that, although the difference between FMA and 3'-TFMA linkages is merely in the substitution of the T6(O3') in the former by a sulfur atom in the latter, the steric and electronic properties resulting from a single-atom substitution can induce significant local structural distortion in an otherwise well-structured oligonucleotide duplex. The NMR parameters described above should allow us to derive high-resolution local structures of the 3'-TFMA-containing segment and establish a model of an unusual backbone conformation that may help to explain the apparent increased stabilization of hybrid DNA · RNA duplexes over their FMA-containing counterparts (Gao et al., 1992).

ACKNOWLEDGEMENTS

We thank Charles Su for technical assistance in carrying out temperature-variable UV meas-

urements, Fred Hassman for providing the unmodified SS ODN sequences and Dr. Robert Jones, John F. Milligan and Mark Matteucci of Gilead Sciences for providing a sample of the 3'-thioformacetal SS ODN used in this study.

REFERENCES

Blommers, M.J., Van de Ven, F.J.M., Van der Marel, G.A. and Van Boom, J.H. (1991) *Eur. J. Biochem.*, **210**, 33–51.

Chandrasekaran, R., Birdsall, D.L., Leslie, A.G.W. and Ratcliff, R.L. (1980) *Nature*, **283**, 743–745.

Chary, K.V.R., Hosur, R.V., Govil, G., Zu-Kun, T. and Miles, H.T. (1988) *Biochemistry*, **26**, 1315–1322.

Cruse, W.B.T., Salisbury, S.A., Brown, T., Cosstick, R., Eckstein, F. and Kennard, O. (1986) *J. Mol. Biol.*, **192**, 891–905.

Dickerson, R.E. (1983) *J. Mol. Biol.*, **166**, 419–441.

Froehler, B.C., Ng, P.G. and Matteucci, M.D. (1986) *Nucleic Acids Res.*, **14**, 5399–5407.

Gao, X. and Burkhart, W. (1991) *Biochemistry*, **30**, 7730–7739.

Gao, X., Brown, F.K., Jeffs, P., Bischofberger, N., Lin, K.-Y., Pipe, A.J. and Noble, S.A. (1992) *Biochemistry*, **31**, 6228–6236.

Gao, X. and Jeffs, P.W. (1994) *J. Biomol. NMR*, in press.

Haasnoot, C.A.G., De Leeuw, F.A.A.M. and Altona, C. (1980) *Tetrahedron*, **36**, 2783–2792.

Heinemann, U., Rudolph, L.-N., Claudia, A., Morr, M., Heikens, R.F. and Blocker, H. (1991) *Nucleic Acids Res.*, **19**, 427–433. This report describes a crystallographic study of a selfcomplementary DNA duplex $d(GCCCG_{CH_2PO_2O}GGC)_2$, in which the 3'-oxygen is substituted by a methylene group. This duplex adopted a deformed A-type conformation with the exception of the modified dG5 which displays C2'-exo (N-type) rather than the C3'-endo conformation of the unmodified residue in the reference sequence. Interestingly, it was found that the restructuring in sugar pucker of the modified dG5 was accompanied by a crankshaft rotation of the α and γ torsion angles of the same residue (in the 5'-direction), resulting in an unusual α(trans)-β(trans)-γ(trans) backbone conformation.

Jones, R.J., Lin, K-Y., Milligan, J.F., Wadwani, S. and Matteucci, M.D. (1993) *J. Org. Chem.*, **58**, 2983–2991.

Katahira, M., Sugeta, H., Kyogoku, Y., Fujii, S., Fujisawa, R. and Tomita, K. (1988) *Nucleic Acids Res.*, **16**, 8619–8632.

Matteucci, M. (1990) *Tetrahedron Lett.*, **31**, 2385–2388.

Matteucci, M. (1991) *Nucleosides and Nucleotides*, **10**, 231–234.

Matteucci, M., Lin, K.-Y., Butcher, S. and Moulds, C.J. (1991) *J. Am. Chem. Soc.*, **113**, 7767–7768.

McBride, L.J. and Caruthers, N.G. (1983) *Tetrahedron Lett.*, **24**, 245–248.

Neuhaus, D. and Williamson, M. (1989) *The Nuclear Overhauser Effect in Structural and Conformational Analysis*, VCH Publishers, New York, NY, pp. 104–110.

Patel, D.J., Shapiro, L. and Hare, D. (1987) *Q. Rev. Biophys.*, **20**, 35–112.

Reid, B.R. (1987) *Q. Rev. Biophys.*, **20**, 1–34.

Saenger, W. (1984) *Principles of Nucleic Acid Structure*, Springer Verlag, New York, NY.

Uhlmann, E. and Peyman, A. (1990) *Chem. Rev.*, **90**, 543–584.

Veal, J. and Brown, F.K. (1992) predicted that the 3'-TFMA-modified sugar prefers a C3'-endo-type conformation as opposed to a C2'-endo by ab-initio quantum mechanics, unpublished results.

Veeneman, G.H., Van der Marel, G.A., Van den Elst, H. and Van Boom, J.H. (1991) *Tetrahedron*, **47**, 1547–1562.

Veeneman, G.H., Van der Marel, G.A., Van den Elst, H. and Van Boom, J.H. (1990) *Recl. Trav. Chim. Pays-Bas*, **109**, 449–451.

Wüthrich, K. (1986) *NMR of Proteins and Nucleic Acids*, Wiley, New York, NY.